IDEA, a CAD Tool for the Design of Deformable Micro-Structures: Extension to the 2D Deformation of Arbitrarily-Shaped Membranes

J. Juillard and E. Colinet
Département SSE, SUPELEC
91192 Gif-sur-Yvette CEDEX, France
jerome.juillard@supelec.fr

ABSTRACT

This paper deals with the extension of a software tool aimed at the design of deformable MEMS structures, from the 1D (axisymmetric) case to the 2D case. This tool is based on an inverse formulation of the nonlinear design problem, which leads to very short computing times compared to classical approaches. In the present paper, we focus on the mechanical part of the inverse problem and validate our approach by comparing with finite element simulations, in the case of a deformable micro-mirror.

Keywords: MEMS design, deformable structures, coupled-field physics, inverse problems, boundary element method, Von Karman equations.

1 INTRODUCTION

This paper deals with the extension from the one-dimensional to the two-dimensional case of an original approach [1] to the design of electrostatically-actuated deformable micro-structures (fig. 1).

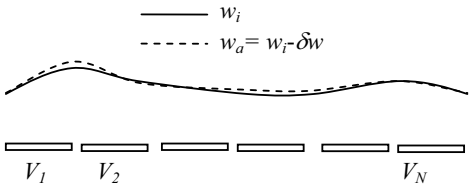

fig. 1: design problem for an electrostatic deformable micro-mirror, as in [2].

The advantage of this approach, as opposed to classical ones (fig. 2), is that typically non-linear coupled problems, such as the large-displacement electrostatic actuation of an elastic plate, are transformed into simple linear non-coupled problems (fig. 3), with a very good accuracy [3]. The complexity of the calculations -and consequently the computing times- are therefore greatly reduced. This approach has been implemented in IDEA, a software tool aimed at the (Inverse) Design of Electrostatic Actuators and, more generally, at the design of actuators involving coupled-field physics and displacement-dependent non-linearities.

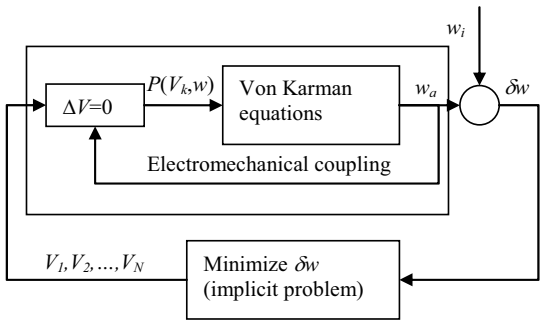

fig. 2: in the classical approach, because of the electromechanical coupling, minimizing the residual displacements is an implicit problem: each call of the optimization loop involves complex non-linear calculations which can only be solved iteratively

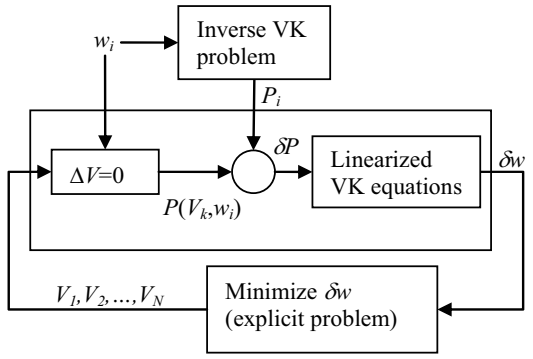

fig. 3: in the inverse approach, the inverse Von Karman problem is solved once and for all outside the optimization loop. The ideal pressure P_0 and stress state corresponding to W_0 are then used to linearize the Von Karman equations. The optimization problem thus becomes explicit.

Our present work focuses on the inversion of the mechanical problem, that is, computing the ideal pressure distribution corresponding to a given set of -supposedly large- displacements. This requires finding a solution to the equations of Von Karman [4] (1) and (2):

$$\frac{Eh^3}{12(1-\nu^2)}\Delta^2 w = P + h\left(\frac{\partial^2 F}{\partial y^2}\frac{\partial^2 w}{\partial x^2} + \frac{\partial^2 F}{\partial x^2}\frac{\partial^2 w}{\partial y^2} - 2\frac{\partial^2 F}{\partial x \partial y}\frac{\partial^2 w}{\partial x \partial y}\right) \quad (1)$$

$$\Delta^2 F = -E\left(\frac{\partial^2 w}{\partial x^2}\frac{\partial^2 w}{\partial y^2} - \left(\frac{\partial^2 w}{\partial x \partial y}\right)^2\right) \quad (2)$$

This problem, which could be treated analytically in the one-dimensional (axisymmetric) case, must be handled numerically in the more general case (two-dimensional deformation of an arbitrarily-shaped membrane). We show how inverting the equations of Von Karman can be achieved by splitting the process in two steps. First, a - possibly analytical- particular solution to a biharmonic problem must be found. This solution is then used as an input to the plane stress problem which corresponds to the homogenous part of the Von Karman equations: this is solved numerically by using a boundary-element approach. Thanks to the good conditioning of the problem, this numerical step does not require any special treatment (as, for example, regularization) and a robust, accurate solution can be obtained without much difficulty (fig. 4). The present paper is mostly devoted to this resolution of the inverse Von Karman problem in a non-trivial geometry, both from a mechanical and from a numerical point of view.

The optimization problem which must be solved in order to obtain the actuation voltages corresponding to the desired shape can then be completely linearized, thanks to the calculated ideal pressure distribution, as in [1].

This method is carefully explained and it is illustrated in the case of the two-dimensional deformation of a continuous deformable micro-mirror, as in [2]. Numerical results obtained with IDEA are given for different sets of displacements and compared with finite element simulations of the direct problem: the pressure distribution calculated with IDEA is input into an ANSYS model of the micro-mirror and the corresponding displacements are then compared to the predicted ones.

2 METHODOLOGY

The initial mechanical problem is the following. Consider a thin plate with interior Ω and boundary Γ. Let Γ_c be the clamped edge(s) of the plate and Γ_f the free edge(s) of the plate. For a plate with uniform thickness h, Young's modulus E and Poisson's coefficient ν, starting from a set of possible displacements w, one can deduce the corresponding pressure P as the solution to (1) and (2).

In order to calculate P from (1), one must first find the solution to (2) which satisfies the following boundary conditions:

$$\begin{cases} U_i(\Gamma_c) = 0 \\ \Sigma_i(\Gamma_f) = 0 \end{cases} \quad (3)$$

Equation (3) merely states that the transverse displacements U_i must be zero on all clamped edges and that the stresses Σ_i must be zero on all free edges.

In order to solve (2) for the Airy stress function, one looks for a solution with the following form:

$$F_i = F_0 + F_{part} \quad (4)$$

F_{part} is a particular solution of (2), with arbitrary boundary conditions. F_0 is a homogenous solution of (2), with nontrivial boundary conditions, that is:

$$\begin{cases} \Delta^2 F_0 = 0 \\ U_0(\Gamma_c) = -U_{part}(\Gamma_c) \\ \Sigma_0(\Gamma_c) = -\Sigma_{part}(\Gamma_c) \end{cases} \quad (5)$$

where U_{part} and Σ_{part} are, respectively, the transverse displacements and stresses corresponding to F_{part}. That way, one ensures that the total solution F_i corresponding to w_i verifies the boundary conditions (3).

2.1 Finding a particular solution

Solving (2) for a particular solution is a simple enough process which can be achieved in a variety of ways. A straightforward approach consists in expressing (2) in a two-dimensional Fourier space:

$$\Delta^2 F_{part} = -E\left(\frac{\partial^2 w}{\partial x^2}\frac{\partial^2 w}{\partial y^2} - \left(\frac{\partial^2 w}{\partial x \partial y}\right)^2\right) = S \quad (6)$$

$$\Leftrightarrow TF_{2D}(F_{part}) = \frac{1}{k^4} TF_{2D}(S)$$

with

$$TF_{2D}(f) = \tilde{f}(k_x, k_y) = \iint_{x,y=-\infty\cdots\infty} f(x,y)\exp(-jk_x x - jk_y y)\,dx\,dy$$

and $k^2 = {k_x}^2 + {k_y}^2$

Using an inverse Fourier transform, one can easily compute F_{part} from (6). F_{part} can then be differentiated in order to calculate the corresponding internal stresses and displacements. Using the definition of the internal stresses [4], it is possible to calculate the components of the stress tensor Σ_{part} at any point.

$$\sigma_{xx}^{part} = \frac{\partial^2 F^{part}}{\partial y^2}, \sigma_{yy}^{part} = \frac{\partial^2 F^{part}}{\partial x^2}, \sigma_{xy}^{part} = -\frac{\partial^2 F^{part}}{\partial x \partial y} \quad (7)$$

Knowing the internal stress state and the prescribed displacements w, one may now use Hooke's law (8) to calculate the transverse displacements U_{part}:

$$\begin{cases} \dfrac{\partial u_x^{part}}{\partial x} = -\dfrac{1}{2}\left(\dfrac{\partial w}{\partial x}\right)^2 + \dfrac{1}{E}\left(\sigma_{xx}^{part} - \nu\sigma_{yy}^{part}\right) \\ \dfrac{\partial u_y^{part}}{\partial y} = -\dfrac{1}{2}\left(\dfrac{\partial w}{\partial y}\right)^2 + \dfrac{1}{E}\left(\sigma_{yy}^{part} - \nu\sigma_{xx}^{part}\right) \\ \dfrac{\partial u_x^{part}}{\partial y} + \dfrac{\partial u_y^{part}}{\partial x} = -\dfrac{\partial w}{\partial x}\dfrac{\partial w}{\partial y} + 2\dfrac{1+\nu}{E}\sigma_{xy}^{part} \end{cases} \quad (8)$$

This can be done by subtracting the second equation from the first. One gets:

$$\begin{cases} \dfrac{\partial u_x^{part}}{\partial x} - \dfrac{\partial u_y^{part}}{\partial y} = -\dfrac{1}{2}\left(\left(\dfrac{\partial w}{\partial x}\right)^2 + \left(\dfrac{\partial w}{\partial y}\right)^2\right) \\ + \dfrac{1+\nu}{E}\left(\sigma_{xx}^{part} - \sigma_{yy}^{part}\right) = S_1 \\ \dfrac{\partial u_x^{part}}{\partial y} + \dfrac{\partial u_y^{part}}{\partial x} = -\dfrac{\partial w}{\partial x}\dfrac{\partial w}{\partial y} + 2\dfrac{1+\nu}{E}\sigma_{xy}^{part} = S_2 \end{cases} \quad (9)$$

By differentiating with respect to x and y, these two equations can be arranged into:

$$\begin{cases} \Delta u_x^{part} = \dfrac{\partial S_1}{\partial x} + \dfrac{\partial S_2}{\partial y} \\ \Delta u_y^{part} = -\dfrac{\partial S_1}{\partial y} + \dfrac{\partial S_2}{\partial x} \end{cases} \quad (10)$$

One can then solve for U_{part} by using a two-dimensional Fourier transform, as above. Now that a particular solution to the second equation of Von Karman has been found, one may look for a solution to the homogenous problem (5).

2.2 Finding a homogenous solution

Equation (5) is equivalent to an interior plane stress problem with prescribed displacements on the boundary. This kind of problem can be classically addressed by using a boundary element method (BEM) [5].

Introducing the tractions t_j on the boundary with outward normal $\vec{n}(n_x, n_y)$, so that:

$$t_i^0 = \sigma_{ij}^0 n_j \quad (9)$$

Somigliana's identity holds for any point P:

$$c(P)u_i^0(P) = \int_\Gamma u_{ij}^*(P,M)t_j^0(M)d\Gamma(M) - \int_\Gamma t_{ij}^*(P,M)u_j^0(M)d\Gamma(M) \quad (10)$$

where

$$\begin{cases} c(P) = 1 \text{ if } P \in \Omega \\ c(P) = 1/2 \text{ if } P \in \Gamma \\ c(P) = 0 \text{ otherwise} \end{cases}$$

and

$$\begin{cases} u_{ij}^*(P,M) = \dfrac{-1}{8\pi(1-\nu')G}\left((3-4\nu')\delta_{ij}\log r - r_{,i}r_{,j}\right) \\ t_{ij}^*(P,M) = \dfrac{-1}{4\pi(1-\nu')r}\left(\begin{matrix}\left((1-2\nu')\delta_{ij} + 2r_{,i}r_{,j}\right)\dfrac{\partial r}{\partial n} \\ -(1-2\nu')\left(r_{,i}n_j - r_{,j}n_i\right)\end{matrix}\right) \end{cases} \quad (11)$$

In (11), G is the shear modulus, ν' is a modified Poisson coefficient[1] and r denotes the distance between point P and point M. The notation δ_{ij} stands for a Kronecker delta and $r_{,j}$ stands for the derivative of r with respect to coordinate j.

[1] $\nu' = \dfrac{\nu}{1+\nu}$

The problem's boundary (e.g. a circle with radius R_0) is then discretized into small panels (the so-called boundary elements) and (10) is approximated using a finite element formulation; by letting point P go to the boundary and writing (10) for every panel node, one obtains a (linear) matrix relationship between the displacements on the boundary (which are known) and the -unknown- tractions on the boundary. This process is rather tedious and the reader is referred to [10] for more details.

The resulting linear system can be solved easily enough and relation (10) can then be used to compute the homogenous solution $\Sigma_0(P)$ and $U_0(P)$ at any point P belonging to Ω.

The total solution can then be obtained from:

$$\begin{cases} U_i(P) = U_0(P) + U_{part}(P) \\ \Sigma_i(P) = \Sigma_0(P) + \Sigma_{part}(P) \end{cases} \quad (12)$$

It is then possible to make use of equation (1) to calculate the pressure corresponding to the prescribed displacements w_i.

3 IMPLEMENTATION

The above treatment of the Von Karman equations has been implemented in IDEA, a Matlab-based graphical software tool.The degrees of freedom for the mechanical part of the problem are the size and geometry of the membrane (including clamped, free or mixed boundary conditions), the material coefficients and, of course, the desired shape. So far, IDEA is restricted to static calculations but its extension to steady-state AC analysis is currently underway. Knowing the ideal pressure distribution corresponding to the input displacements, IDEA can then be used to compute the voltage distributions that yield the "best" approximation to the desired shape: this requires a special treatment [1] [3] because of the non-negativity constraints imposed by the electrostatic forces. However, the pressure output by the mechanical part may be used "as is" in the case of piezoelectric actuation, for example [6]. The implementation of the mechanical inverse problem is pretty straightforward in itself. The input displacements are defined on a finite difference grid with $2^N \times 2^M$ nodes, so as to get the best performance out of the fast Fourier transforms that are necessary for obtaining the particular solution of (2). The boundary element method is then used: the membrane's boundary is decomposed into small flat panels and a Gaussian quadrature scheme - with adjustable accuracy - is used for evaluating the integrals resulting from (10). Since the panels are flat, the singular integrals corresponding to the influence of each panel on itself can be expressed analytically. The total running time for this calculation is on the order of 1 second using a PC with a 2.8GHz CPU and 760 Mo RAM[2].

4 VALIDATION

We validate our approach and its implementation by comparing our results with those obtained with ANSYS.

[2] The same computer is used for the ANSYS calculations in the following section.

We consider a circular membrane with a 15mm radius and a 1μm thickness, as the micro-mirror appearing in [2]. The material properties are E=170 GPa, ν=0.3. The same approach as in [3] is used: the ideal pressure distributions corresponding to different input shapes are first calculated using IDEA. These pressure distributions are then input into an equivalent ANSYS model of the membrane; the displacements resulting from the finite element calculation can then be compared to the initial shape.

In the following examples, we have used:

$$w_i(r,\theta) = W_0 \frac{r^4}{{R_0}^4}\left(1-\frac{r^2}{{R_0}^2}\right)^2 \sin\theta \qquad (13)$$

W_0 takes two values: 5×10^{-7} and 5×10^{-5}, respectively corresponding to maximum displacement values of 3.12×10^{-2}μm and 3.12μm. The first case should then be bending dominated, whereas the second case should be membrane dominated. For both examples, the same finite difference grid is used with 256×256 nodes and the membrane boundary is discretized into 128 elements. The ANSYS model is composed of about 10^4 SHELL63 elements. The input displacement shape and the corresponding pressure distributions calculated with IDEA are shown in fig. 4, as well as the mismatch between IDEA input and ANSYS output. In all the tested cases, the error is less than 1%, thereby validating our approach. Finally, we would like to stress the point that the solution time for the direct problem with ANSYS is on the order of 10-100 times the solution time for the inverse problem, depending on how nonlinear the problem is: in our opinion, this emphasizes the huge benefit that can be drawn from inverse modeling techniques in the context of MEMS design and simulation.

REFERENCES

[1] J. Juillard, M. Cristescu, "An inverse approach to the design of adaptive micro-mirrors", Journal of Micromechanics and Microengineering, vol. 14, pp. 347-355, 2003

[2] G. Vdovin, P.M. Sarro, "Flexible mirror micro-machined in silicon", Applied Optics, vol. 34, (16), pp. 2968-2972, 1995

[3] J. Juillard et al., "Finite element validation of an inverse approach to the design of an electrostatic actuator", Nanotech 2004, vol. 2, pp. 275-278, 2004

[4] E. Landau, E. Lifschitz, "Théorie de l'élasticité", Physique Théorique, tome 7, Mir, Moscou, 1967

[5] P.J. Hunter, A.J. Pullan, "FEM/BEM Notes", University of Oakland, New Zealand, 2003

[6] T.G. Bifano et al., "Microelectromechanical Deformable Mirrors", Journal of Selected Topics in Quantum Electronics, (5), pp. 83-90, 1999

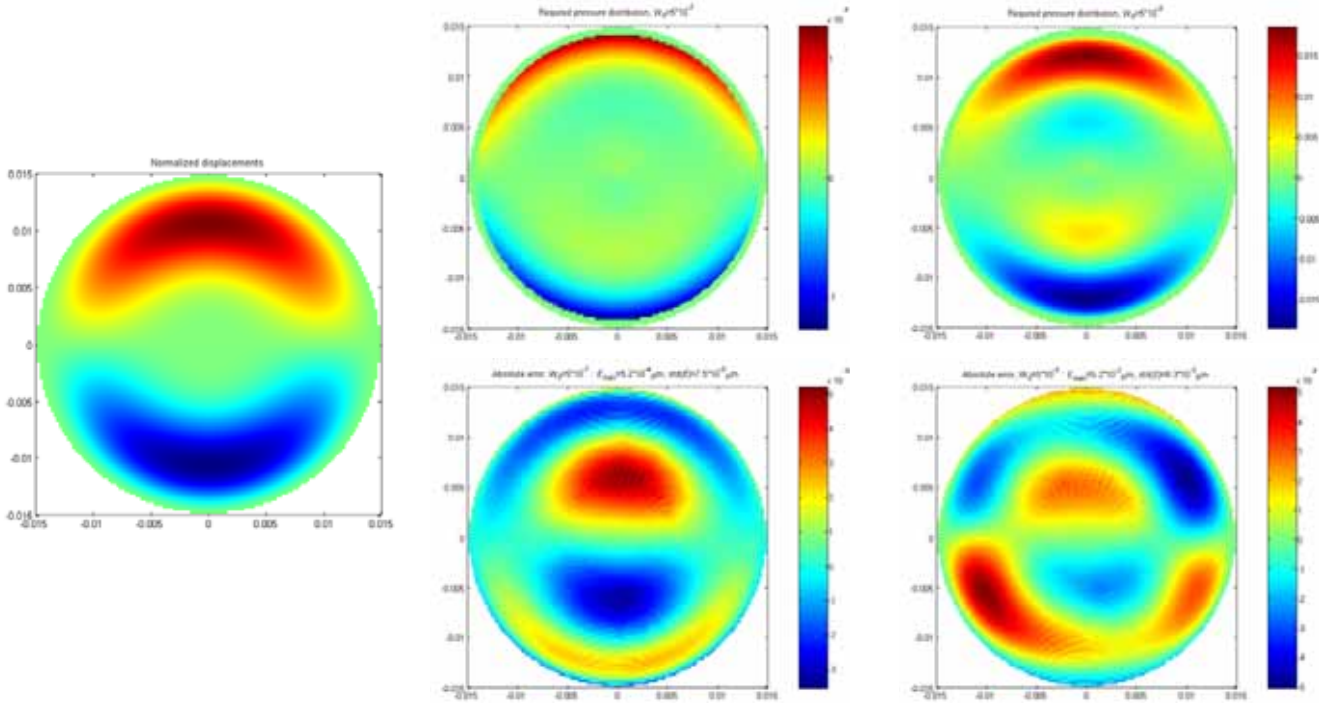

fig. 4: for the normalized displacement shape (13) - left column- IDEA outputs the pressure distributions (top line) for W_0=5×10^{-7} (left) and 5×10^{-5} (right). The corresponding errors obtained by subtracting the ANSYS results from (13) are represented in the bottom line for W_0=5×10^{-7} (left) and 5×10^{-5} (right). In both cases, the maximum of the error is about 2% of the maximum displacement value and the standard deviation is about 2‰ of the maximum displacement value.